BIOCHEMISTRY
including biophysical chemistry & molecular biology

ARTICLE

pubs.acs.org/biochemistry

Effect of the Y955C Mutation on Mitochondrial DNA Polymerase Nucleotide Incorporation Efficiency and Fidelity

Patricia A. Estep and Kenneth A. Johnson*

Department of Chemistry and Biochemistry, Institute for Cellular and Molecular Biology, The University of Texas, 2500 Speedway, Austin, Texas 78712, United States

ABSTRACT: The human mitochondrial DNA polymerase (pol γ) is responsible for the replication of the mitochondrial genome. Mutation Y955C in the active site of pol γ results in early onset progressive external ophthalmoplegia, premature ovarian failure, and Parkinson's disease. In single-turnover kinetic studies, we show that the Y955C mutation results in a decrease in the maximal rate of polymerization and an increase in the K_m for correct incorporation. The mutation decreased the specificity constant for correct incorporation of dGTP, TTP, and ATP to values of 1.5, 0.35, and 0.044 μM^{-1} s^{-1}, respectively, representing reductions of 30-, 110-, and 1300-fold, respectively, relative to the value for the wild-type enzyme. The fidelity of incorporation was reduced 6−130-fold, largely because of the significant decrease in the specificity constant for correct dATP:T incorporation. For example, k_{cat}/K_m for forming a TTP:T mismatch was decreased 10-fold from 0.0002 to 0.00002 μM^{-1} s^{-1} by the Y955C mutant, but the 1300-fold slower incorporation of the correct dATP:T relative to that of the wild type led to a 130-fold lower fidelity. While correct incorporation of 8-oxo-dGTP was largely unchanged, the level of incorporation of 8-oxo-dG with dA in the template strand was reduced 500-fold. These results support a role for Y955 in stabilizing A:T base pairs at the active site of pol γ and suggest that the severe clinical symptoms of patients with this mutation may be due, in part, to the reduced efficiency of incorporation of dATP opposite T, and that the autosomal dominant phenotype may arise from the resulting higher mutation frequency.

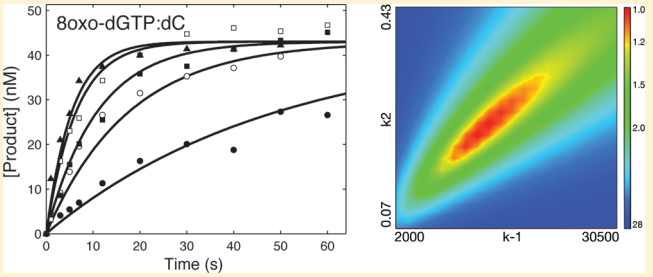

Understanding the molecular basis for disease has become an increasingly important part of biochemical studies as genetic testing becomes more common. Identification of the proteins or genes responsible for a particular disease could allow for better treatments and/or earlier intervention. Deletions or mutations in human mitochondrial DNA polymerase (pol γ) have been correlated with various mitochondrial disorders, including mtDNA depletion syndrome, Alpers syndrome, and progressive external ophthalmoplegia (PEO).[1] Symptoms of Alpers syndrome include liver disease and refractory seizures, while patients with PEO present with progressive weakness of the external ocular muscles and skeletal myopathy.[2,3]

Mitochondrial DNA (mtDNA) replication is performed by a replisome comprised of a nuclearly encoded catalytic subunit, two subunits of the processivity factor (p55), the single-stranded DNA binding protein, and a DNA helicase.[4] The crystal structure of the holoenzyme, a heterotrimer comprised of the catalytic subunit of the polymerase and a dimer of p55, was recently determined.[5] Like those of other family A polymerases, the mtDNA polymerase structure resembles a right hand comprised of thumb, fingers, and palm domains. Recent studies of two other family A polymerases, HIV reverse transcriptase and T7 DNA polymerase, have guided our work on pol γ, providing insight into the mechanism of catalysis as well as the potential mechanisms of discrimination against incorrect nucleotides and the role of nucleotide-induced conformational changes in selectivity.[6,7] The pathway of nucleotide incorporation can be simplified to that shown in Scheme 1

$$ED_n + N \overset{K_d}{\rightleftarrows} ED_nN \overset{k_{pol}}{\rightleftarrows} ED_{n+1} + PP_i \qquad \text{(Scheme1)}$$

where ED_n represents a complex of enzyme with DNA that is n bases long and N represents a nucleoside triphosphate. In this simplified scheme, ground-state binding is represented by the term $1/K_1$ (K_d), while the rate of chemistry is described by k_{pol}. Normally, pyrophosphate release and translocation to allow the binding of the next nucleotide are much faster than incorporation.[8−10] The rate of incorporation measured in a single-turnover experiment defines the kinetics governing sequential nucleotide incorporation events during processive synthesis. Accordingly, the values of k_{pol}/K_d measured in single-turnover kinetic studies define k_{cat}/K_m for processive synthesis. Moreover, the apparent K_d measured in these studies should be more generally described as a K_m value, which approaches a true K_d when the chemistry step is slow.[6,7] Throughout this work, we will refer to the results from our single-turnover kinetic studies in

Received: February 23, 2011
Revised: June 21, 2011
Published: June 22, 2011

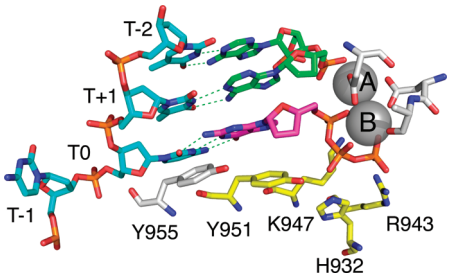

Figure 1. Position of Y955 at the polymerase active site. Residue Y955 is colored white. The incoming nucleotide is colored magenta. The template strand is colored cyan and the primer green. Active site residues with homology to residues in the T7 DNA polymerase structure are shown on the basis of the structure of the T7 DNA polymerase ternary complex[11] (Protein Data Bank entry 1T7P) with residue numbers corresponding to the pol γ structure.

terms of k_{cat} and K_m values to eliminate the misconception that the results define K_d.

The crystal structure of the ternary complex of pol γ has yet to be determined, so comparisons between pol γ and T7 DNA polymerase have been helpful in identifying the potential roles of particular residues. As summarized in Figure 1, catalytic residues are conserved in comparing T7 DNA polymerase and pol γ, thereby allowing homology modeling based upon the T7 DNA polymerase ternary E−DNA−nucleotide complex[11,12] to suggest possible interactions at the active site. Within the active site of pol γ, homology suggests that residue R943 contacts the γ-phosphate, while Y951 and H932 each contact the β-phosphate, leaving K947 to make contact with the α-phosphate, as confirmed by recent mutagenesis studies.[13] Tyrosine 955 is not involved directly in contacts with the phosphate backbone; rather, it appears that it participates in a hydrogen bonding network involving a glutamate residue in the palm of the enzyme [E895 in pol γ (not shown)]. This hydrogen bond network may be essential not only for maintaining the architecture of the polymerase active site but also for the recognition of the correct incoming nucleotide. Mutation of Y530 to a phenylalanine in T7 DNAP resulted in a loss of discrimination through a lower affinity for the incoming nucleotide rather than a decrease in the rate of polymerization.[14]

Autosomal dominant forms of PEO usually involve mutations in pol γ that are in the active site of the polymerase. Patients with the Y955C mutation present with early onset autosomal dominant PEO in their thirties.[15] These patients often later present with Parkinson's disease and, in women, premature ovarian failure.[15−17] MtDNA in skeletal muscle cells of these patients shows some deletions, though a large proportion of the mtDNA is intact, indicating some level of complete replication by the polymerase.[17] In yeast, a mutant of Mip1 homologous to the human polymerase γ mutant Y955C leads to increased petite frequency, suggesting mitochondrial malfunction.[18] In addition, qualitative studies have shown that both the mutation and deletion frequency are increased with this mutant.[3,19]

Oxidatively damaged guanosine, in the form of 8-oxodeoxyguanosine (8-oxo-dG), accumulates in the mitochondria and contributes to the formation of mutations.[20] The 8-oxo-dG can base pair with either a cytosine in the *anti* conformation or an adenosine in the *syn* conformation, leading to frequent mutations.[21] pol γ uses a novel mechanism to reduce the rate of incorporation of 8-oxo-dGTP by slowing the rate of pyrophosphate release, allowing the chemical reaction to come to equilibrium at the enzyme active site.[21] It is important to establish which residues are responsible for this slow pyrophosphate release, as they affect discrimination against 8-oxo-dGTP. Therefore, we have examined the kinetics of incorporation by the Y955C mutant as part of this study. Moreover, if the Y955C mutant incorporated 8-oxo-dGTP at a higher rate, that could account for the observed physiological effects of this mutation.

Understanding the molecular basis for diseases linked to mtDNA replication requires accurate kinetic analysis for quantification of the effects of the mutation. Although many mutations in pol γ have been characterized previously,[12,22,23] we show in this study that the published results are unreliable. Our new results provide a basis for correlating the biochemistry of mtDNA replication with physiology.

MATERIALS AND METHODS

Cloning and Plasmid Construction for the Large Subunit of Polymerase γ (p140). The creation of the Y955C mutant on an exonuclease deficient background (D198A/E200A) on the pUC19 plasmid (New England Biolabs) was performed using two-step polymerase chain reaction (PCR) using primers flanking SacII and NotI restriction sites. The following mutagenic primers were used: 5′ CAA TTA CGG TCG TAT TTG CGC GCA GGT CAG CCG 3′ and complementary strand 5′ GCT GAC CTG CGC CGC AAA TAC GAC CGT AAT TGA AAA T 3′. The SacII and NotI restriction sites were used to insert the PCR-generated fragment into the gene. A NotI/BglII digest was then used to remove the gene from pUC19.1 for ligation into the pBacPak9 vector (Clontech). Creation of baculovirus containing the gene for Y955C pol γ was previously described.[13]

Purification of Small Subunit (p55) and Polymerase γ Y955C Mutants. The small subunit (p55) was expressed using the pET43.1a vector with a histidine tag in *Escherichia coli* Rosetta 2 (DE3) and then purified as previously described.[13] For purification of the large subunit of the polymerase with the Y955C mutation, the cells were lysed by resuspension in a buffer containing 0.32 M sucrose, 10 mM HEPES (pH 7.5), 3 mM $CaCl_2$, 2 mM $MgAc\cdot 4H_2O$, and 0.1 mM EDTA. Protease Inhibitor Cocktail IV (EDTA-free, AG Scientific) was added to the lysis buffer. The lysate was clarified by centrifugation at 1500*g* for 15 min. DNA was removed by increasing the level of salt to a final KCl concentration of 0.5 M. The lysate was again centrifuged in a Beckman Coulter ultracentrifuge at 31000*g* in a Ti45 rotor. Next, the lysate was subjected to a Ni-NTA column (QIAgen) via the batch method. The protein was bound to the resin pre-equilibrated with 20 mM HEPES (pH 7.5), 5 mM imidazole, 200 mM KCl, and 5% glycerol by being stirred on ice. The beads were collected via centrifugation at 1500*g* for 10 min and then washed with 20 mM HEPES (pH 7.5), 200 mM KCl, 20 mM imidazole, and 5% glycerol. The beads were then poured into a column, and the protein was eluted with 20 mM HEPES (pH 7.5), 100 mM KCl, 200 mM imidazole, and 5% glycerol. The fractions containing the polymerase were pooled and diluted before being loaded onto an SP Sepharose column (Amersham Biosciences) at a flow rate of 1 mL/min in buffer A consisting of 20 mM HEPES (pH 7.5), 30 mM KCl, 1 mM DTT, 1 mM EDTA, and 5% glycerol. Buffer B consisted of 20 mM HEPES (pH 7.5), 700 mM KCl, 1 mM DTT, 1 mM EDTA, and 5% glycerol. The protein was eluted with a step gradient from 0 to 100% B. The fractions containing pol γ were pooled, concentrated via a centrifugal concentrator with a 50 kDa cutoff (GE Healthcare), and dialyzed against the final storage

Table 1. Primer and Template Sequences Used for Single-Turnover Experiments[a]

oligo	number of nucleotides	sequence
primer	25	5′ GCCTCGCAGCCGTCCAACCAACTCA 3′
template 1	45	5′ GGACGGCATTGGATCGAGGTTGAGTTGGTTGGACGGCTGCGAGGC 3′
template 2	45	5′ GGACGGCATTGGATCGAGTCTGAGTTGGTTGGACGGCTG CGAGGC 3′
template 3	45	5′ GGACGGCATTGGATCGAGTATGAGTTGGTTGGACGGCTGCGAGGC 3′

[a] The length is given in nucleotides. The underlined base is the templating base for the incoming nucleotide.

buffer consistng of 50 mM Tris-HCl (pH 8.4), 100 mM NaCl, 1 mM DTT, and 50% glycerol. Concentrations of the active enzyme were obtained by active site titration of the burst amplitude versus DNA concentration.

Preparation of DNA. Oligonucleotides were purchased from IDT DNA Technologies and purified using 15% acrylamide−7 M urea denaturing polyacrylamide gel electrophoresis (PAGE) gels. A 25-mer primer and a 45-mer template (template 1 shown in Table 1) were adopted from previous studies for misincorporation assays.[13] Templates 2 and 3 were used for incorporation assays involving 8-oxo-dGTP. The 25-mer was 5′ labeled with ^{32}P with T4 polynucleotide kinase as recommended by the manufacturer (New England Biolabs). Excess [γ-^{32}P]ATP was removed with a Bio-Spin 6 gel filtration column (Bio-Rad), and the amount of labeled DNA was quantified by TLC. The labeled 25-mer and unlabeled 45-mer were mixed in a 1:1 molar ratio and annealed by being heated to 95 °C for 5 min and then slowly cooled to room temperature.

Single-Turnover Experiments. All experiments were performed at 37 °C in a solution containing 50 mM Tris-HCl (pH 7.5), 100 mM NaCl, and 12.5 mM $MgCl_2$. To eliminate complications from multiple turnovers, reactions were performed under single-turnover conditions, with enzyme in excess and limiting DNA substrate. For fast reactions, assays were performed with a KinTek RQF-3 Rapid Quench Flow apparatus. For both correct incorporation and misincorporation assays, the holoenzyme (200−300 nM large subunit and 0.8−1.2 μM small subunit) was preincubated with 25/45-mer DNA (140−200 nM) in reaction buffer without magnesium chloride and loaded into one syringe. The other syringe contained the nucleotide (0.5−500 μM for correct incorporation and 25 μM to 5 mM for incorrect incorporation) in reaction buffer with magnesium chloride. After the sample had been rapidly mixed, the reaction was quenched with 0.5 M EDTA. Misincorporation assays requiring longer periods of time were performed by manual mixing. Reactions involving 8-oxo-dGTP were performed with either rapid quenching or hand quenching with 8-oxo-dGTP concentrations varying from 1 μM to 1 mM.

The products were resolved on 15% acrylamide−/7 M denaturing PAGE gels. The gels were dried and exposed to a PhosphorImager screen. The screen was then scanned with a Typhoon Scanner (GE Healthcare Life Sciences) to reveal product bands. The amount of product (26-mer) was quantified versus the amount of starting material to determine the fraction of product.

Global Fitting. All data were fit globally on the basis of numerical integration of rate equations using KinTek Explorer (KinTek Corp.).[24,25] Nonlinear regression was used to find optimal parameters in fitting each set of data to a single model. While data were being fit, previously estimated rates of DNA binding and release were used in constructing a comprehensive model including all known steps. For example, Scheme 1 was expanded to

$$E + D_n \underset{k_{off}}{\overset{k_{on}}{\rightleftarrows}} ED_n$$

$$ED_n + N \underset{k_{-1}}{\overset{k_1}{\rightleftarrows}} ED_nN \overset{k_2}{\rightleftarrows} ED_{n+1} + PP_i$$

The DNA binding and dissociation rates for both substrate and product DNA (D_n and D_{n+1}, respectively) were set to 20 μM^{-1} s^{-1} (k_{on}) and 0.02 s^{-1} (k_{off}) to satisfy the steady-state DNA release rate and the $K_{d,DNA}$ of 10 nM.[26] The rate of nucleotide binding is thought to be limited by diffusion, so k_1 was set to 100 μM^{-1} s^{-1}. By allowing the dissociation rate to vary (k_{-1}), we calculated the equilibrium constant ($K_1 = k_1/k_{-1}$). Thus, to fit a full concentration series, only k_{-1} and k_2 were adjusted to fit the family of curves and thereby define the apparent K_d (K_m) and k_{pol} (k_{cat}), respectively. To account for slight variations in the data, the enzyme or DNA concentration was adjusted slightly (±10%) to derive best fits. Standard error estimates were obtained by nonlinear regression and were checked using confidence contour analysis. The upper and lower limits were derived on the basis of a χ^2 threshold of 20%, as previously described.[25] In all cases, the error estimates derived by nonlinear regression were similar to the estimates based upon the confidence contour analysis, verifying that the parameters were well constrained.

In presenting the results in each of the figures, we omitted data for long periods of time from the graph to illustrate more clearly the data for shorter periods of time. Although not displayed, data for longer periods of time were included in the data fitting. In particular, the points for longer periods of time help to define the amplitude of the reactions at the lower concentrations as part of the global fitting.

Note on Nomenclature. We reserve the term "rate constant" to refer to an "intrinsic rate constant" for an individual step in a reaction pathway (i.e., that represented by a lowercase k over an arrow). We see little utility in the distinction between a rate derived by an initial velocity (slope as the change in product with time) and a rate measured by fitting to an exponential function and do not adhere to the standard that the latter should be termed a "rate constant". Although clearly having distinct meanings and units, both are methods for measuring the rate of a reaction. Moreover, it is often misleading to presume that an eigenvalue derived by fitting data to an exponential function is an intrinsic rate constant. In the process of fitting data, we derive rates of reaction in units of s^{-1}, and because these measurements do not necessarily resolve individual rate constants, we refer to them as rate measurements.

Free Energy of Discrimination. Discrimination against each mismatch was calculated from

$$D = \frac{(k_{cat}/K_m)_{correct}}{(k_{cat}/K_m)_{mismatch}}$$

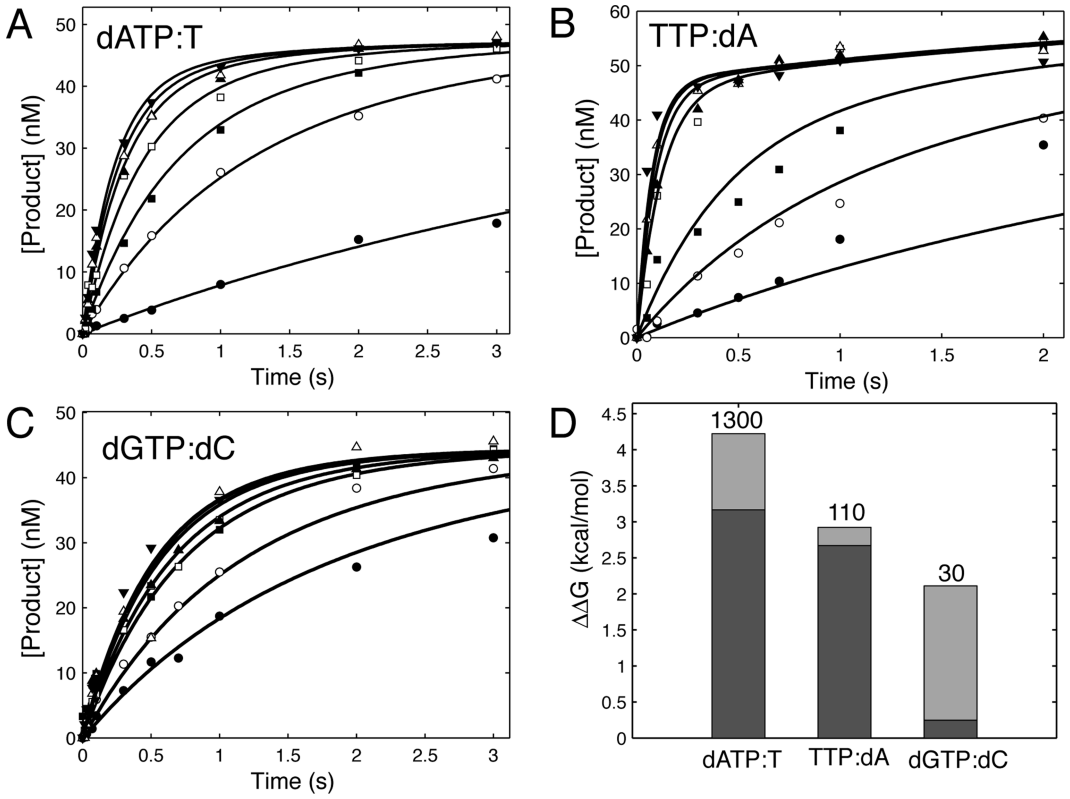

Figure 2. Kinetics of correct base pair incorporation. For each experiment, a preformed enzyme−DNA complex was rapidly mixed with Mg^{2+} and various concentrations of dATP, dCTP, dGTP, or TTP. In each experiment, the final concentrations of the enzyme and DNA after mixing were 100−150 and 70 nM, respectively. In the global fitting of each data set, the concentration of active enzyme was adjusted slightly to fit the amplitude. (A) Incorporation of a dATP:T base pair into Y955C exo− pol γ at 5 (●), 25 (○), 50 (■), 100 (□), 200 (▲), 300 (△), and 500 μM (▼) was globally fit to yield a k_{cat} of 5.4 ± 0.45 s^{-1} and a K_m of 120 ± 15 μM. (B) Formation of a TTP:dA base pair with the Y955C exo− pol γ at various concentrations of TTP [1 (●), 3 (○), 7 (■), 50 (□), 100 (▲), 200 (△), and 300 μM (▼)] was globally fit to Scheme 1 to yield a k_{cat} of 16.6 ± 3.1 s^{-1} and a K_m of 46 ± 11 μM. (C) Formation of a dGTP:dC base pair with Y955C exo− pol γ at various concentrations of dGTP [0.5 (●), 1 (○), 3 (■), 5 (□), 15 (▲), 50 (△), and 150 μM (▼)] was globally fit to yield a k_{cat} of 1.8 ± 0.18 s^{-1} and a K_m of 1.2 ± 0.32 μM. (D) Change in the specificity constant for each correct base pair incorporation relative to the wild type on a free energy scale. The numbers above each bar give the fold change in k_{cat}/K_m in comparing the wild type with the Y955C mutant. Contributions arising from k_{cat} (light gray) and K_m (dark gray) were calculated as described in Materials and Methods.

which is equal to the reciprocal of the frequency of misincorporation (fidelity). We computed the apparent change in free energy due to the Y955C mutation reflected in the changes in k_{cat} and K_m using the following equations:

$$\Delta\Delta G_c = -RT \ln\left(\frac{k_{cat}^{Y955C}}{k_{cat}^{wt}}\right)$$

$$\Delta\Delta G_m = -RT \ln\left(\frac{K_m^{wt}}{K_m^{Y955C}}\right)$$

The net change in the specificity constant is the sum of the contributions from k_{cat} and K_m on the free energy scale.

Calculation of k_{cat} and K_m. After fitting data in Figure 5C to Scheme 2, we computed k_{cat} and K_m from the following:

$$k_{cat} = \frac{k_2 k_3}{k_2 + k_{-2} + k_3}$$

$$K_m = \frac{k_2 k_3 + k_{-1}(k_{-2} + k_3)}{k_1(k_2 + k_{-2} + k_3)}$$

$$k_{cat}/K_m = k_1 \frac{k_2 k_3}{k_2 k_3 + k_{-1}(k_{-2} + k_3)}$$

RESULTS

Kinetics of Single-Nucleotide Incorporation Measured by Quench-Flow Experiments. Single-nucleotide incorporation experiments were performed to determine the parameters for correct nucleotide incorporation by the Y955C mutant. The experiments were performed under single-turnover conditions in that the concentration of enzyme exceeded the concentration of DNA. The nucleotide concentration dependence of the rate was analyzed to provide estimates of an apparent dissociation constant ($K_{d,app} = K_m$) and a maximal rate of nucleotide incorporation ($k_{pol} = k_{cat}$) according to Scheme 1. Figure 2 shows the time dependence of product formation at several nucleotide

dx.doi.org/10.1021/bi200280r |*Biochemistry* 2011, 50, 6376–6386

Table 2. Effect of pol γ Y955C on the Kinetics of Correct Base Pair Incorporation[a]

	base pair	k_{cat} (s^{-1})	K_m (μM)	k_{cat}/K_m ($\mu M^{-1}\ s^{-1}$)	*x*-fold effect
Y955C	dATP:T	5.4 ± 0.45	120 ± 15	0.044 ± 0.006	1300
	dGTP:dC	1.8 ± 0.18	1.2 ± 0.3	1.5 ± 0.4	30
	TTP:dA	17 ± 3	46 ± 11	0.35 ± 0.1	110
WT[b]	dATP:T	45 ± 1	0.8 ± 0.06	57 ± 5	
	dGTP:dC	37 ± 2	0.8 ± 0.12	46 ± 7	
	TTP:dA	25 ± 2	0.6 ± 0.16	40 ± 10	

[a] Kinetic parameters were derived in fitting the data in Figure 2. The *x*-fold effect on k_{cat}/K_m was calculated from values for the wild type divided by the k_{cat}/K_m from the mutant. [b] Values for the wild type were previously determined.[28]

concentrations for defining the kinetics of incorporation of dATP:T, dGTP:dC, and TTP:dA mismatches. To avoid confusion, we use the notation dATP:T to represent the incorporation of dATP opposite a template T, for example. The data in the experiment were globally fit to the mechanism shown in Scheme 1 based upon numerical integration of the rate equations, yielding values for the apparent nucleotide dissociation constant and the maximal rate of incorporation.[24]

Several underlying assumptions govern the fitting of the data to the model in Scheme 1. Ground-state nucleotide binding is thought to occur as a rapid equilibrium, which was modeled with the initial collision of the nucleotide and enzyme occurring at a rate limited by diffusion (100 $\mu M^{-1}\ s^{-1}$) to define an apparent dissociation constant, $K_{d,app}$ (K_m). Second, the rate-limiting step is believed to be polymerization, while conformational changes preceding chemistry, pyrophosphate release, and translocation are thought to be fast, based upon more detailed studies of homologous enzymes.[6,7] Accordingly, the $k_{pol}/K_{d,app}$ ratio defines k_{cat}/K_m, the specificity constant governing sequential nucleotide incorporation events during processive synthesis.

The kinetic parameters for correct incorporation are summarized in Table 2 and compared to the values for the wild-type enzyme.[27] The Y955C mutation affected not only the rate of polymerization, decreasing by a factor of as much as 20, but also k_{cat}/K_m. The effect on k_{cat}/K_m was most severe with dATP:T base pairs, mostly because of much weaker nucleotide binding. As summarized in Table 2, the Y955C mutation caused a 1300-fold reduction in k_{cat}/K_m for incorporation of the dATP:T base pair, while the effects on TTP:dA and dGTP:dC base pairs were only 110- and 30-fold, respectively.

Kinetics of Misincorporation. The kinetics of misincorporation were measured to investigate the discrimination against mismatches by the Y955C mutant compared to the wild-type enzyme. In particular, we examined the incorporation of dCTP, TTP, and dGTP opposite a templating T. In many cases, multiple nucleotides were incorporated onto the primer strand such that products up to 32 nucleotides long were observed (see Figure 3). When the product was quantified, all of the extended primers were included in the total concentration of product formed to define the rate of formation of the first mismatch. The concentration of product was plotted as a function of time (Figure 4) and then fit globally to Scheme 1, yielding the kinetic parameters listed in Table 3. The kinetic parameters for misincorporation for the wild-type enzyme were determined previously[28] and are listed for comparison. As shown in Table 3, there is a significant

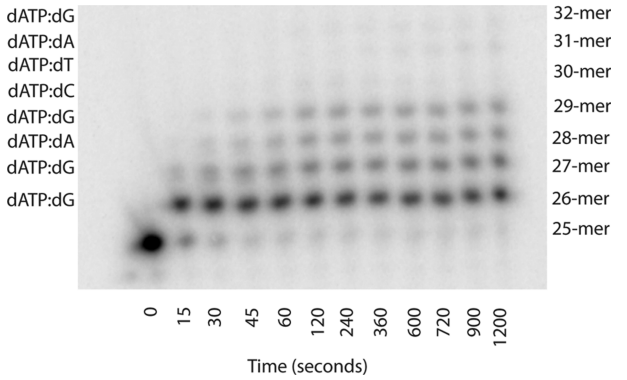

Figure 3. Multiple misincorporation events. Products from misincorporation of dGTP (at 1000 μM) onto a templating T catalyzed by Y955C exo− pol γ were separated on a 15% acrylamide−7 M urea denaturing PAGE gel to visualize the formation of multiple misincorporation products over time. The text on the left gives the identity of the dNTP and template corresponding to each incorporation. For example, dATP:dG refers to misincorporation of dATP opposite dG in the template.

decrease in fidelity, 6-, 26-, 120-, and 50-fold for dGTP:T, dCTP:T, TTP:T, and dGTP:dA mismatches, respectively.

Incorporation of 8-oxo-dGTP. The kinetics of incorporation of 8-oxo-dGTP were measured under single-turnover conditions opposite a dCMP or dAMP templating base. The formation of product over time is shown in panels A and B of Figure 5 and fit to Scheme 1, yielding the results summarized in Table 4. These data show no significant change in k_{cat}/K_m for incorporation of 8-oxo-dGTP opposite a template dC, but a 500-fold reduction for incorporation opposite a template dA, compared to that of the wild type.

It was important to evaluate whether the kinetics of incorporation of 8-oxo-dGTP followed the more complex pattern seen with the wild-type enzyme. That is, with the wild-type enzyme the kinetics show a clear nucleotide concentration dependence of amplitude as shown in Figure 5C, reproduced from ref 21. Incorporation of 8-oxo-dGTP by the wild-type enzyme follows Scheme 2, with a slow pyrophosphate release leading to accumulation of the product complex ($ED_{n+1}PP_i$) in equilibrium with bound substrate. This leads to a distinct kinetic signature in which the amplitude of the pre-steady-state burst is dependent upon nucleotide concentration.

$$ED_n + N \overset{K_d}{\rightleftarrows} ED_nN \underset{k_{-2}}{\overset{k_2}{\rightleftarrows}} ED_{n+1}PP_i \qquad \text{(Scheme2)}$$

$$ED_{n+1}PP_i \overset{k_3}{\rightleftarrows} ED_{n+1} + PP_i$$

In Figure 5C, we reproduce the data from ref 21 but now fit the data globally to the model shown in Scheme 2. Confidence contour analysis (Figure 6B) justifies the fitting of the data to four rate constants by showing that all four rate constants are well constrained.

Incorporation of 8-oxo-dGTP opposite a templating dC by the Y955C mutant (Figure 5B) does not show the same pattern seen for the wild-type enzyme. That is, the curves for the Y955C mutant share the same end point derived by fitting the data globally, and the model shown in Scheme 1 can sufficiently account for the data. Thus, unlike that of the wild-type enzyme (Figure 5C), the concentration dependence of incorporation of 8-oxo-dGTP by the mutant gave no evidence to suggest that the reaction was followed

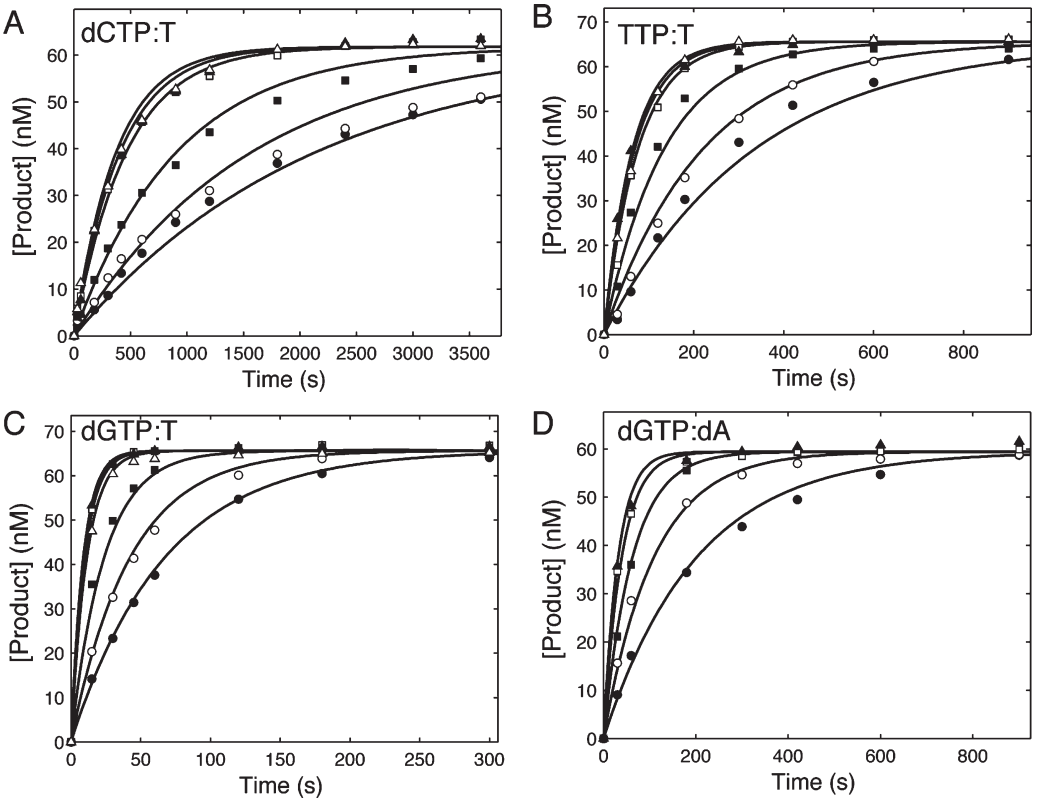

Figure 4. Kinetics of misincorporation. For each experiment, a preformed enzyme−DNA complex ([enzyme] > [DNA duplex]) was rapidly mixed with Mg^{2+} and various concentrations of nucleotide. In each experiment, the final concentrations of the enzyme and DNA after mixing were 100−150 and 70 nM, respectively. In the global fitting of each data set, the concentration of active enzyme was adjusted slightly to fit the amplitude. (A) Formation of a dCTP:T mismatch by Y955C exo− pol γ at 300 (●), 500 (○), 1000 (■), 3000 (□), 4000 (▲), and 5000 μM (△) was fit globally to yield a k_{cat} of 0.004 ± 0.002 s^{-1} and a K_m of 2020 ± 148 μM. (B) Formation of a TTP:T mismatch by Y955C exo− pol γ at each concentration of TTP [300 (●), 500 (○), 1000 (■), 3000 (□), 4000 (▲), and 5000 μM (△)] was globally fit to yield a k_{cat} of 0.022 ± 0.0050 s^{-1} and a K_m of 1360 ± 138 μM. (C) Formation of a dGTP:T mismatch by Y955C exo− pol γ at each concentration of dGTP [300 (●), 500 (○), 1000 (■), 3000 (□), 4000 (▲), 5000 and μM (△)] was globally fit to yield a k_{cat} of 0.22 ± 0.024 s^{-1} and a K_m of 2950 ± 397 μM. (D) Formation of a dGTP:dA base pair with Y955C exo− pol γ [25 (●), 50 (○), 100 (■), 200 (□), and 300 μM (▲)] was globally fit to Scheme 1 to yield a k_{cat} of 0.064 ± 0.014 s^{-1} and a K_m of 217.1 ± 31.18 μM. In each panel, the smooth lines show the fitted curves derived by global fitting using KinTek Explorer.[24,25]

Table 3. Effect of the Y955C Mutation of Kinetic Parameters Governing Fidelity[a]

	base pair	k_{cat} (s^{-1})	K_m (μM)	k_{cat}/K_m (μM^{-1} s^{-1})	D
Y955C	dATP:T	5.4 ± 0.45	120 ± 15	0.044 ± 0.0064	–
	dGTP:T	0.22 ± 0.02	3000 ± 400	0.00008 ± 0.00001	550
	dCTP:T	0.004 ± 0.002	2020 ± 150	0.000002 ± 0.000001	22000
	TTP:T	0.022 ± 0.0050	1360 ± 140	0.00002 ± 0.000004	2200
	dGTP:dA	0.06 ± 0.01	220 ± 30	0.0003 ± 0.00006	7500
WT[b]	dATP:T	45 ± 1	0.8 ± 0.06	56 ± 4	–
	dGTP:T	1.16 ± 0.06	70 ± 10	0.16 ± 0.003	3500
	dCTP:T	0.038 ± 0.003	360 ± 80	0.001 ± 0.00002	570000
	TTP:T	0.013 ± 0.0003	57 ± 5	0.0002 ± 0.00002	260000
	dGTP:dA	<0.1	>1000	0.0001	390000

[a] Kinetic parameters were derived in fitting the data in Figure 4. Discrimination (D) was calculated as the ratio of k_{cat}/K_m values for correct vs mismatched base pairs. [b] Values for the wild-type enzyme were determined previously.[27,28]

by slow pyrophosphate release. The rate of misincorporation of an 8-oxo-dGTP:dA base pair by the Y955C mutant was 500-fold slower [k_{cat}/K_m = 0.0004 μM^{-1} s^{-1} (Table 4)] than the rate of misincorporation by the wild type (k_{cat}/K_m = 0.2 μM^{-1} s^{-1}), and thus, the mutant exhibited an increased level of discrimination against misincorporation of 8-oxo-dGTP. The rate of incorporation of 8-oxo-dGTP:dA was comparable to the rate of misincorporation of dGTP:dA [k_{cat}/K_m = 0.0003 μM^{-1} s^{-1} (Table 3)].

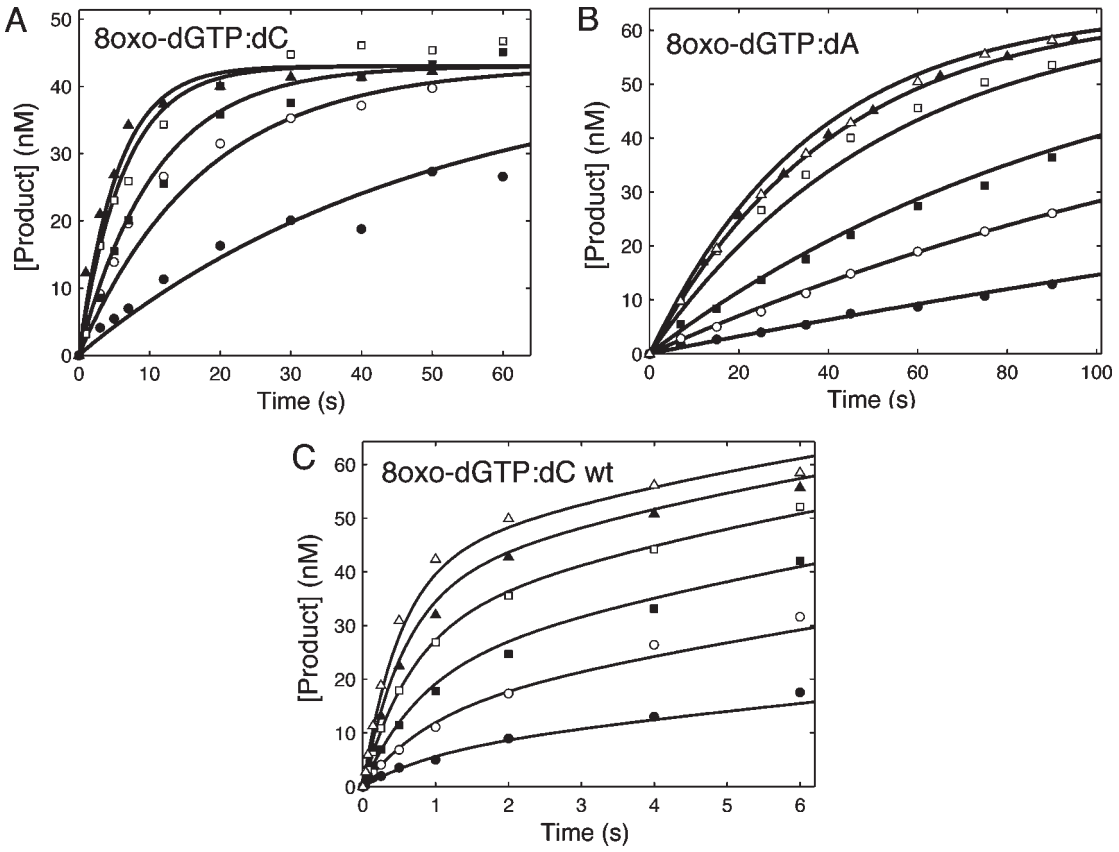

Figure 5. Kinetics of incorporation of 8-oxo-dGTP. For each experiment, a preformed enzyme−DNA complex ([enzyme] > [DNA duplex]) was rapidly mixed with Mg^{2+} and various concentrations of TTP, dGTP, or 8-oxo-dGTP. In each experiment, the final concentrations of the enzyme and DNA after mixing were 100−150 and 70 nM, respectively. In the global fitting of each data set, the concentration of active enzyme was adjusted slightly to fit the amplitude. (A) Formation of the 8-oxo-dG:dC base pair with Y955C exo− pol γ at various concentrations of 8-oxo-dGTP [5 (●), 15 (○), 50 (■), 100 (□), 300 (▲), and 500 μM (△)] was globally fit to Scheme 1 to yield a k_{cat} of 0.28 ± 0.049 s^{-1} and a K_m of 163 ± 42.1 μM. (B) Formation of the 8-oxo-dG:dA base pair with Y955C exo− pol γ at various concentrations of 8-oxo-dGTP [10 (●), 25 (○), 50 (■), 150 (□), 300 (▲), and 500 μM (△)] was globally fit to Scheme 1 to yield a k_{cat} of 0.035 ± 0.005 s^{-1} and a K_m of 95 ± 11 μM. (C) Formation of the 8-oxo-dG:dC base pair [10 (●), 25 (○), 50 (■), 100 (□), 200 (▲), and 400 μM 8-oxo-dGTP (△)] with wild-type exo− pol γ fit globally to Scheme 2 to derive the following: $K_{d,1}$ = 135 ± 15 μM, k_2 = 1.6 ± 0.14 s^{-1}, k_{-2} = 0.7 ± 0.15 s^{-1}, and k_3 = 0.23 ± 0.06 s^{-1}. Data are from ref 21. In each panel, the smooth lines show the fitted curves derived by global fitting using KinTek Explorer.[24,25] Data fitting by conventional means provided the following estimates: $K_{d,1}$ = 135 μM, k_2 = 2 s^{-1}, k_{-2} = 0.7 s^{-1}, and k_3 = 0.4 s^{-1}.[21] Thus, the rate constants derived by both methods are comparable, but the confidence in the fitting derived by simulation is greater because it includes both rate and amplitude data in a single fitting step rather than a complex combination of plots of rate and amplitudes as a function of concentration.

Overall, the data suggest that the physiological effects of the Y955C mutation are not due to increased rates of incorporation of 8-oxo-dGTP.

Global Fitting and Contour Analysis. Each set of curves was globally fit using KinTek Explorer.[24,25] The global fitting routine is based on numerical integration of rate equations, allowing the parameters to be derived by being directly fit to a complete model. In this type of fitting, both the rate and the amplitude of the reaction are taken into account, eliminating the simplifications of equations and errors that are common during traditional fitting. This has proven to be useful in fitting data for which there is a clear nucleotide concentration dependence of the amplitude, or data for which the nucleotide concentration is comparable to that of the enzyme. It is necessary to ensure that the model is not overly complex, and that the data are able to support the definition of each step in the model. We address this by performing confidence contour analysis, whereby the constants are systematically varied, and we estimate the extent to which each parameter in a model is constrained by the data.

In contour analysis (Figure 6A), the red zone represents a range of values that provide a good fit to the data given in Figure 5A. The margin shown by the yellow band between the red and green zones defines a boundary that represents a 20% increase in χ^2, which is used to estimate the upper and lower confidence intervals for each of the parameters.[25] In the case of incorporation of 8-oxo-dGTP by the Y955C mutant (Figure 5A), we can see that the parameters are well constrained by the data to support the mechanism shown in Scheme 1. The upper and lower confidence limits have been compared to the standard error estimates derived by nonlinear regression. Because the two methods of estimating errors agreed for the data reported here, we omitted the upper and lower limits from the tables for the sake of clarity. Note also that the k_{cat}/K_m ratio is known with greater certainty than either parameter, k_{cat} or K_m, as revealed by the linear relationship between k_2 and k_{-1} on the confidence contour. This is equivalent to stating that the slope of a rate versus concentration curve is known with greater certainty than the k_{cat}/K_m value computed from the ratio of the k_{cat} and K_m values.

Table 4. Effect of the pol γ Y955C Mutation on Incorporation of 8-oxo-dGTP[a]

	base pair	k_{cat} (s^{-1})	K_m (μM)	k_{cat}/K_m ($\mu M^{-1}\ s^{-1}$)	*x*-fold effect
Y955C	8-oxo-dGTP:dC	0.28 ± 0.05	160 ± 40	0.002 ± 0.0005	1.5
	8-oxo-dGTP:dA	0.035 ± 0.005	95 ± 11	0.0004 ± 0.00007	500
WT	8-oxo-dGTP:dC	0.15 ± 0.02	48 ± 8	0.003 ± 0.001	
	8-oxo-dGTP:dA[b]	0.62 ± 0.05	3.3 ± 1.0	0.20 ± 0.1	

[a] Values for k_{cat} and K_m were calculated from the individual rate constants as described in Materials and Methods. [b] Values taken from ref 21.

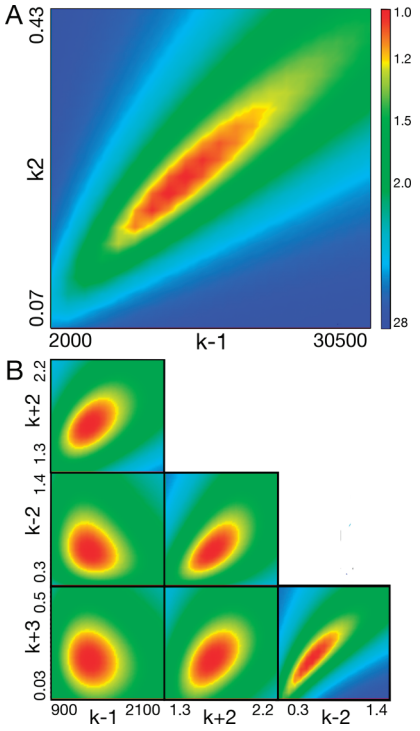

Figure 6. Confidence contours. (A) Relationship between the total χ^2 and the two kinetic parameters, k_2 (k_{cat}) and k_{-1} ($K_m = k_{-1}/k_1$), with the color scale ranging from red (best fit) to blue. The scale is based upon the ratio of χ^2 divided by the minimal χ^2. A threshold at 1.2 provides upper and lower limits for each parameter[25] defined by the yellow band. Note that the ratio of the two parameters (defining k_{cat}/K_m) is known with greater certainty than either parameter individually. (B) Confidence contours for fitting data in Figure 5C from ref 21. The color scale is identical to that in panel A. The contours demonstrate that all four parameters are well constrained.

In Figure 6B, we show the confidence contours derived from global fitting of the data in Figure 5C. This analysis demonstrates that all four rate constants were well constrained in fitting the data to Scheme 2 based upon simultaneously fitting the rate and amplitude dependence of the observed reaction. As summarized in the legend of Figure 5, the rate constants derived by global fitting are comparable to those obtained by conventional analysis; however, the error limits are better defined by the global fitting, and the concentration dependencies of the rate and amplitude are fit simultaneously, rather than separately.

DISCUSSION

In all family A polymerases, there is a tyrosine residue at the end of the helix containing several catalytic residues. Studies involving the T7 DNA polymerase have suggested that this residue plays a role in stabilizing the incoming nucleotide, with the phenyl ring of the tyrosine stacking with the nucleotide, and the hydroxyl group forming hydrogen bonds that help to stabilize the architecture of the active site.[11] Mutation of the homologous residue (Y530) to phenylalanine in T7 DNA polymerase resulted in an increase in the dissociation constant for incoming nucleotides with an only modest effect on the rate of polymerization[14] and a corresponding decrease in fidelity. As shown here, the mutation of tyrosine to a cysteine has a much more drastic effect. In particular, we observe a 30−1300-fold reduction in k_{cat}/K_m governing correct base pair incorporation due to the Y955C mutation. In addition, there was a 6−120-fold reduction in fidelity. In contrast, there was little change in the kinetics of incorporation of 8-oxo-dGTP opposite a template dC, but a 500-fold improvement in discrimination against an 8-oxo-dGTP:dA mismatch.

Previous studies of the Y955C mutation based upon steady-state methods in the Copeland laboratory have provided inconsistent results.[12,29] For example, steady-state measurements gave a k_{cat} of 0.05 s^{-1}, a K_m of 40 nM, and a k_{cat}/K_m of 1.2 $\mu M^{-1}\ s^{-1}$ for incorporation of a dGTP:dC base pair by the wild-type enzyme.[30] In contrast, our methods provided a k_{cat} of 37 s^{-1}, a K_m of 0.8 μM, and a k_{cat}/K_m of 46 $\mu M^{-1}\ s^{-1}$ (Table 2). Thus, the specificity constant derived by steady-state methods was 38-fold lower than what we observed in single-turnover experiments. Comparing values for the wild-type enzyme and the Y955C mutant reveals that the k_{cat}/K_m values derived by steady-state methods in the Copeland laboratory were lower by factors ranging from 27- to 62000-fold[30] compared to the results presented here. Most noteworthy is the fact that Copeland and his co-workers underestimated the rate of incorporation of 8-oxo-dGTP:dA by the wild-type enzyme by a factor of 8000-fold and thus failed to properly assess the importance of mismatch formation with this oxidatively damaged nucleotide. In addition, they underestimated the specificity constant for incorporation of a dGTP:dC base pair by the Y955C mutation by 62000-fold and accordingly overstated the magnitude of the defect. Similar discrepancies exist in the specificity constants for incorporation of nucleoside analogues used to treat HIV infections in comparing the results from pre-steady-state[31] and steady-state kinetics.[32] Via comparison of the published results from two papers from the Copeland lab,[12,29] the k_{cat} value for the wild-type enzyme was reported to be either 0.36 min^{-1} or 1.3 s^{-1}. This 220-fold variation in k_{cat} values reported for the wild-type enzyme engenders little confidence in the quality of the data.

For DNA polymerases, steady-state k_{cat} and K_m values are reduced by a factor approaching the processivity of the enzyme, which for pol γ is approximately 2000.[26] Although, in theory, steady-state measurements on DNA polymerases should still provide a valid specificity constant[33] and may be adequate for enzymes with low processivity,[34] in practice, experiments with pol γ would need to be designed to accurately measure a steady-

state K_m value of ~0.5 nM to accurately assess correct incorporation kinetics. As a counterargument, one might propose that the single-turnover kinetics overestimate the rates because the first turnover might be faster than subsequent turnovers. However, experiments for measuring the kinetics of sequential nucleotide incorporation on several DNA polymerases have shown that the rate of incorporation of each nucleotide is comparable to that measured in single-turnover experiments.[9,27,35] Moreover, there is no evidence of a kinetically significant step between sequential nucleotide incorporation events, implying that pyrophosphate release and translocation are normally much faster than incorporation. Direct measurements of pol γ demonstrated that pyrophosphate release was kinetically correlated with incorporation, implying fast pyrophosphate release after chemistry.[36,37] Thus, the rate constants derived from single-turnover kinetic studies accurately define the parameters governing sequential nucleotide incorporation events during processive synthesis and prevent the complications introduced in steady-state measurements of a processive DNA polymerase. Moreover, pre-steady-state experiments provide important quality control for the concentration of active enzyme in a preparation from the measured amplitude of the reaction. After a survey of the literature about pol γ, it is our opinion that the results of steady-state kinetics, in general, and those from the Copeland lab, in particular, are unreliable and conclusions based upon their quantitative results must be reevaluated.

Family A polymerases typically have a two-step binding mechanism, in which a conformational change is a critical component of nucleotide recognition.[6,7,38] Studies of T7 DNA polymerase and HIV RT have shown that this conformational change is fast and establishes the specificity constant for correct incorporation. However, when the chemistry step is slow, the conformational change comes to equilibrium before incorporation.[6,7] Without any method for measuring the conformational change in pol γ, it is difficult to interpret whether the apparent K_d represents a true dissociation constant or simply reflects the ratio of k_{cat} and the net substrate binding rate. The issue is whether the binding steps come to equilibrium before the chemistry step. In either case, the apparent K_d provides an accurate estimate of the K_m governing single-nucleotide incorporation during processive synthesis and k_{pol}/K_d defines the specificity constant, k_{cat}/K_m.[6,7] In studies of T7 DNA polymerase and HIV RT, it was shown that when the rate of chemistry is reduced by mutation or when a mismatch or a nucleoside analogue is incorporated, the binding steps come to equilibrium.[6,7] Accordingly, the slow rate of incorporation suggests that binding comes to equilibrium with the Y955C mutation, implying a significant effect of the Y955C mutation on nucleotide binding (Figure 2 and Table 2).

The Y955C mutation resulted in a reduced rate of polymerization and a decrease in the k_{cat}/K_m for correct incorporation. The effect of the mutation on the maximal rates of polymerization varied from 1.5- to 20-fold for correct incorporation (Table 2). However, the catalytic efficiencies (k_{cat}/K_m) were reduced 30−1300-fold. Thus, the effect of the Y955C mutation on the chemistry step was less significant and not correlated with the largest changes in k_{cat}/K_m. In particular, the specificity constant for incorporation of dATP:T was reduced 1300-fold with an only 8-fold reduction in k_{cat}. Thus, unlike that of the wild-type enzyme, the specificity constant varied considerably for different base pairs. Perhaps the hydrogen bond network involving this tyrosine in the wild-type enzyme compensates for fewer hydrogen bonds in forming an A:T base pair compared to a G:C base pair, as suggested in early work on T7 DNA polymerase.[14] Perhaps the stacking interaction between the tyrosine and the incoming base acts as an equalizer, allowing the rates of binding and polymerization to be less dependent on the type and size of the base. Cysteine is unable to compensate. Because of the positioning of Y955 (on the O-helix in T7 DNA polymerase), the interaction with the E895 residue may be critical in the ground-state binding of the incoming nucleotide. The hydroxyl group of the tyrosine may stabilize the carboxyl group of the glutamate in the active site. In the T7 DNA polymerase, this glutamate selectively stabilizes the incoming TTP of a T:A base pair.[14] This interaction may be reflected in Y955C pol γ as an increased K_m for TTP or dATP and reduced rates of catalysis.

Another significant detrimental effect of the Y955C mutation is reduced fidelity. The largest decrease in fidelity occurred between a T:T mismatch from one error in 260000 for the wild type compared to one in 2200 for the Y955C mutant. This 120-fold decrease in fidelity may contribute to the physiological consequences of this mutation. While replicating DNA, the Y955C mutant slows when reaching a T in the template, and one time in 2200 it will incorporate a T:T mismatch. We show that the Y955C mutant catalyzes multiple misincorporation events, unlike the wild-type enzyme, which is perhaps equally important.[27]

We have also studied the kinetics of incorporating 8-oxo-dGTP opposite dC and dA in the template. Our single-turnover experiments suggest not only that there is a low level of discrimination against 8-oxodeoxyguanosine but also that the level of discrimination is greater against an 8-oxo-dGTP:dA misincorporation (Table 4) for Y955C than for the wild-type enzyme. The wild-type enzyme has an unusual mechanism for minimizing incorporation of 8-oxo-dGTP opposite a dCMP base, creating an equilibrium by slowing the release of pyrophosphate and allowing time for the reverse reaction to compete with product release.[21] This resulted in a nucleotide dependence of amplitude, ultimately slowing the k_{cat} (Figure 5C). However, with the Y955C mutation, there was no evidence of the slow pyrophosphate release, but the level of discrimination is lowered because of weaker nucleotide binding.

Physiological Effects. The Y955C mutation leads to an autosomal dominant phenotype, but the effects are delayed in onset. Although it is termed "early onset PEO", symptoms do not appear until the patients are in their thirties. Thus, mtDNA replication is sufficient for individuals to live normally but then develop symptoms later in life. It is perhaps surprising that such drastic effects on the kinetics of incorporation are not lethal. Here we can only speculate about the relationship between the enzymology of pol γ and the physiological consequences of mutations. We presume that both the mutant polymerase and a wild-type polymerase are present in the same mitochondrion, and perhaps mechanisms that regulate mtDNA copy number somehow compensate for the defective polymerase by allowing the wild-type enzyme to do most of the replication. Nonetheless, the drastic effects on catalytic efficiency and fidelity could ultimately cause the large deletions that are present in mtDNA in PEO patients by slowing the rate of replication such that replication stalls at long T tracts.[16,17,39] More importantly, perhaps, mutations introduced by the defective enzyme would be passed on to subsequent generations of mtDNA replication. Accordingly, it is possible that defects leading to reduced fidelity are more important than defects leading to slower rates of polymerization. While feedback mechanisms could compensate for reduced rates, mutations introduced during each round of replication accumulate over time

and could explain the delayed onset of the disease. Increased mutation frequency can lead to defects in mtDNA that lead to increased oxidative stress, which in turn could lead to an increased level of accumulation of defects in the mtDNA. The accumulation of mutations may result in more severe symptoms such as Parkinson's and premature ovarian failure.[17,29] The dual expression of both Y955C and wild-type polymerase allows for some level of faithful replication and likely prevents all out failure of mtDNA replication.

A recent report noted phenomena suggesting that the replication complex stalls at A:T tracts.[39] Our results provide quantitative data to support the proposed slower rate of replication at dATP:T base pairs. However, simple stalling of the replication complex may not produce the observed physiological effects if other regulatory mechanisms compensate for the reduced number of active replisomes. Alternatively, stalled intermediates could lead to the accumulation of deletions in the mtDNA. Further studies of the polymerase need to be conducted in the presence of the complete replisome to fully understand these dynamics.

AUTHOR INFORMATION

Corresponding Author

*Department of Chemistry and Biochemistry, Institute for Cellular and Molecular Biology, The University of Texas, Austin, TX 78712. E-mail: kajohnson@mail.utexas.edu. Phone: (512) 471-0434. Fax: (512) 471-0435.

Funding Sources

This work was supported by a grant from the National Institutes of Health (GM044613) and by the Welch Foundation (F-1604).

ACKNOWLEDGMENT

KinTek Corp. provided the RQF-3 rapid quench-flow instrument and KinTek Explorer.

ABBREVIATIONS

PEO, progressive external ophthalmoplegia; pol γ, mitochondrial DNA polymerase; mtDNA, mitochondrial DNA.

REFERENCES

(1) Taylor, R. W., and Turnbull, D. (2005) Mitochondrial DNA Mutations in Human Disease. *Nat. Rev. 6*, 14.

(2) Wong, L. J., Naviaux, R. K., Brunetti-Pierri, N., Zhang, Q., Schmitt, E. S., Truong, C., Milone, M., Cohen, B. H., Wical, B., Ganesh, J., Basinger, A. A., Burton, B. K., Swoboda, K., Gilbert, D. L., Vanderver, A., Saneto, R. P., Maranda, B., Arnold, G., Abdenur, J. E., Waters, P. J., and Copeland, W. C. (2008) Molecular and clinical genetics of mitochondrial diseases due to POLG mutations. *Hum. Mutat. 29*, E150–E172.

(3) Lewis, W., Day, B. J., Kohler, J. J., Hosseini, S. H., Chan, S. S., Green, E. C., Haase, C. P., Keebaugh, E. S., Long, R., Ludaway, T., Russ, R., Steltzer, J., Tioleco, N., Santoianni, R., and Copeland, W. C. (2007) Decreased mtDNA, oxidative stress, cardiomyopathy, and death from transgenic cardiac targeted human mutant polymerase. *Lab. Invest. 87*, 9.

(4) Kaguni, L. S. (2004) DNA polymerase γ, the mitochondrial replicase. *Annu. Rev. Biochem. 73*, 293–320.

(5) Lee, Y. S., Kennedy, W. D., and Yin, Y. W. (2009) Structural insight into processive human mitochondrial DNA synthesis and disease-related polymerase mutations. *Cell 139*, 312–324.

(6) Tsai, Y. C., and Johnson, K. A. (2006) A new paradigm for DNA polymerase specificity. *Biochemistry 45*, 9675–9687.

(7) Kellinger, M. W., and Johnson, K. A. (2010) Nucleotide-dependent conformational change governs specificity and analog discrimination by HIV reverse transcriptase. *Proc. Natl. Acad. Sci. U.S.A. 107*, 7734–7739.

(8) Johnson, K. A. (1993) Conformational coupling in DNA polymerase fidelity. *Annu. Rev. Biochem. 62*, 685–713.

(9) Kati, W. M., Johnson, K. A., Jerva, L. F., and Anderson, K. S. (1992) Mechanism and fidelity of HIV reverse transcriptase. *J. Biol. Chem. 267*, 25988–25997.

(10) Johnson, K. A. (2010) The kinetic and chemical mechanism of high-fidelity DNA polymearases. *Biochim. Biophys. Acta 1804*, 1041–1048.

(11) Doublie, S., Tabor, S., Long, A. M., Richardson, C. C., and Ellenberger, T. (1998) Crystal structure of a bacteriophage T7 DNA replication complex at 2.2 Å resolution. *Nature 391*, 251–258.

(12) Graziewicz, M. A., Longley, M. J., Bienstock, R. J., Zeviani, M., and Copeland, W. C. (2004) Structure-function defects of human mitochondrial DNA polymerase in autosomal dominant progressive external ophthalmoplegia. *Nat. Struct. Mol. Biol. 11*, 770–776.

(13) Batabyal, D., McKenzie, J. L., and Johnson, K. A. (2010) Role of histidine 932 of the human mitochondrial DNA polymerase in nucleotide discrimination and inherited disease. *J. Biol. Chem. 285*, 34191–34201.

(14) Donlin, M. J., and Johnson, K. A. (1994) Mutants Affecting Nucleotide Recognition by T7 DNA Polymerase. *Biochemistry 33*, 9.

(15) Van Goethem, G., Martin, J. J., and Van Broeckhoven, C. (2002) Progressive external ophthalmoplegia and multiple mitochondrial DNA deletions. *Acta Neurol. Belg. 102*, 39–42.

(16) Luoma, P. T., Luo, N., Loscher, W. N., Farr, C. L., Horvath, R., Wanschitz, J., Kiechl, S., Kaguni, L. S., and Suomalainen, A. (2005) Functional defects due to spacer-region mutations of human mitochondrial DNA polymerase in a family with an ataxia-myopathy syndrome. *Hum. Mol. Genet. 14*, 1907–1920.

(17) Pagnamenta, A. T., Taanman, J. W., Wilson, C. J., Anderson, N. E., Marotta, R., Duncan, A. J., Bitner-Glindizicz, M., Taylor, R. W., Laskowski, A., Thorburn, D. R., and Rahman, S. (2006) Dominant inheritance of premature ovarian failure associated with mutant mitochondrial DNA polymerase gamma. *Hum. Reprod. 21*, 6.

(18) Baruffini, E., Lodi, T., Dallabona, C., Puglisi, A., Zeviani, M., and Ferrero, I. (2006) Genetic and chemical rescue of the *Saccharomyces cerevisiae* phenotype induced by mitochondrial DNA polymerase mutations associated with progressive external ophthalmoplegia in humans. *Hum. Mol. Genet. 15*, 9.

(19) Ponamerev, M. V., Longley, M. J., Nguyen, D., Kunkel, T. A., and Copeland, W. C. (2002) Active Site Mutation in DNA Polymerase γ Associated with Progressive External Opthalmoplegia Causes Error-prone DNA synthesis. *J. Biol. Chem. 277*, 3.

(20) Pursell, Z. F., McDonald, J. T., Mathews, C. K., and Kunkel, T. A. (2008) Trace amounts of 8-oxo-dGTP in mitochondrial dNTP pools reduce DNA polymerase γ replication fidelity. *Nucleic Acids Res. 36*, 7.

(21) Hanes, J. W., Thal, D. M., and Johnson, K. A. (2006) Incorporation and replication of 8-oxo-deoxyguanosine by the human mitochondrial DNA polymerase. *J. Biol. Chem. 281*, 36241–36248.

(22) Longley, M. J., Graziewicz, M. A., Bienstock, R. J., and Copeland, W. C. (2005) Consequences of mutations in human DNA polymerase γ. *Gene 354*, 125–131.

(23) Copeland, W. C. (2004) Consequences of mutations in DNA polymerase γ. *Environ. Mol. Mutagen. 44*, 193–193.

(24) Johnson, K. A., Simpson, Z. B., and Blom, T. (2009) Global Kinetic Explorer: A new computer program for dynamic simulation and fitting of kinetic data. *Anal. Biochem. 387*, 20–29.

(25) Johnson, K. A., Simpson, Z. B., and Blom, T. (2009) FitSpace Explorer: An algorithm to evaluate multidimensional parameter space in fitting kinetic data. *Anal. Biochem. 387*, 30–41.

(26) Johnson, A. A., Tsai, Y. C., Graves, S. W., and Johnson, K. A. (2000) Human mitochondrial DNA polymerase holoenzyme: Reconstitution and characterization. *Biochemistry 39*, 1702–1708.

(27) Johnson, A. A., and Johnson, K. A. (2001) Fidelity of nucleotide incorporation by human mitochondrial DNA polymerase. *J. Biol. Chem. 276*, 38090–38096.

(28) Lee, H. R., and Johnson, K. A. (2006) Fidelity of the human mitochondrial DNA polymerase. *J. Biol. Chem. 281*, 36236–36240.

(29) Graziewicz, M., Bienstock, R. J., and Copeland, W. C. (2007) The DNA polymerase γ Y955C disease variant associated with PEO and parkinsonism mediates the incorporation and translesion synthesis opposite 7,8-dihydro-8-oxo-2′-deoxyguanosine. *Hum. Mol. Genet. 16*, 10.

(30) Graziewicz, M. A., Bienstock, R. J., and Copeland, W. C. (2007) The DNA polymerase γ Y955C disease variant associated with PEO and parkinsonism mediates the incorporation and translesion synthesis opposite 7,8-dihydro-8-oxo-2′-deoxyguanosine. *Hum. Mol. Genet. 16*, 2729–2739.

(31) Johnson, A. A., Ray, A. S., Hanes, J., Suo, Z. C., Colacino, J. M., Anderson, K. S., and Johnson, K. A. (2001) Toxicity of antiviral nucleoside analogs and the human mitochondrial DNA polymerase. *J. Biol. Chem. 276*, 40847–40857.

(32) Lim, S. E., and Copeland, W. C. (2001) Differential incorporation and removal of antiviral deoxynucleotides by human DNA polymerase γ. *J. Biol. Chem. 276*, 23616–23623.

(33) Boosalis, M. S., Petruska, J., and Goodman, M. F. (1987) DNA polymerase insertion fidelity. Gel assay for site-specific kinetics. *J. Biol. Chem. 262*, 14689–14696.

(34) Bertram, J. G., Oertell, K., Petruska, J., and Goodman, M. F. (2010) DNA polymerase fidelity: Comparing direct competition of right and wrong dNTP substrates with steady state and pre-steady state kinetics. *Biochemistry 49*, 20–28.

(35) Patel, S. S., Wong, I., and Johnson, K. A. (1991) Pre-Steady-State Kinetic Analysis of Processive DNA Replication Including Complete Characterization of an Exonuclease-Deficient Mutant. *Biochemistry 30*, 511–525.

(36) Hanes, J. W., and Johnson, K. A. (2008) Real-time measurement of pyrophosphate release kinetics. *Anal. Biochem. 372*, 125–127.

(37) Hanes, J. W., and Johnson, K. A. (2007) A novel mechanism of selectivity against AZT by the human mitochondrial DNA polymerase. *Nucleic Acids Res. 35*, 6973–6983.

(38) Johnson, K. A. (2008) Role of induced fit in enzyme specificity: A molecular forward/reverse switch. *J. Biol. Chem. 283*, 26297–26301.

(39) Atanassova, N., Fuste, J. M., Wanrooij, S., Macao, B., Goffart, S., Backstrom, S., Farge, G., Khvorostov, I., Larsson, N. G., Spelbrink, J. N., and Falkenberg, M. (2011) Sequence-specific stalling of DNA polymerase γ and the effects of mutations causing progressive ophthalmoplegia. *Hum. Mol. Genet. 20*, 1212–1223.